Journal of Minerals and Materials Characterization and Engineering, 2024, 12, 281-298
https://www.scirp.org/journal/jmmce
ISSN Online: 2327-4085
ISSN Print: 2327-4077

A Model of Physico-Mechanical Characterization of Sangaredi Bauxites and Related Rocks Taking into Account Their Litho-Genetic Type

Oumar Keita[1], Mory Diane[2]

[1]Department of Hydrology, University of Nzérékoré, Nzérékoré, Guinea
[2]Guinea Bauxite Company, Kamsar, Guinea
Email: oumar20003@yahoo.fr, okeita.uz@gmail.com, mory.diane2014@gmail.com

How to cite this paper: Keita, O. and Diane, M. (2024) A Model of Physico-Mechanical Characterization of Sangaredi Bauxites and Related Rocks Taking into Account Their Litho-Genetic Type. *Journal of Minerals and Materials Characterization and Engineering*, **12**, 281-298.
https://doi.org/10.4236/jmmce.2024.126018

Received: September 6, 2024
Accepted: October 13, 2024
Published: October 16, 2024

Abstract

The Sangarédi bauxite deposit in the Republic of Guinea contains several bauxite types depending on their litho-genetics. For rational and sustainable exploitation, determining the physical and mechanical properties of these different bauxite types is essential for mining companies. This paper presents a model for the physico-mechanical characterization of Sangarédi bauxites according to their litho-genetic type. Eight pits were drilled, and samples were collected from different layers at different depth intervals for each bauxite type. Physical and mechanical characterization tests were then carried out on 27 samples to determine the following parameters: water of absorption (%), compressive strength (kgf/cm^2) and dynamic tensile strength (kgf/cm^2). The effect of depth of sampling on these physico-mechanical parameters was evaluated. An average value of the parameters was made for each bauxite type. The results showed that the physico-mechanical characteristics of bauxites depend on the depth of sample collection, and the average value of the parameters constitutes the representative values of the bauxite type. Finally, a comparative study of the average value of the physico-mechanical parameters of the different bauxite types was carried out.

Keywords

Bauxites, Litho-Genetics, Physico-Mechanical, Compressive Strength, Dynamic Tensile Strength

1. Introduction

Guinea has the world's largest bauxite reserves. With a high alumina content,

Guinean bauxites are estimated to be over 40 billion tons, of which 23 billion tons are located in the Boke region [1]. The mining sector is important to the country's economy; it represents 75% to 85% of resources exports by year, especially bauxite [2]. In recent times, several mining companies have been established in Guinea for bauxite exploitation. For miners, the physico-mechanical characterization of bauxites is an important phase because it conditions their exploitation process.

During the last two decades, relevant research has been intensified in many bauxite-producing countries [3]-[6]. Bauxite strength characteristics under different soaking conditions were determined in [3]. [7] and [8] determined the physical and mechanical properties of epoxy-bauxite mortar for High-Friction Surface Treatment (HFSTS). [9] presents an overview of chemical analyses and test results on the physical and strength properties of bauxite residue worldwide. [10] Carried out some research on recycling bauxite waste for the Mineral Industry: Phase Transformations and Microstructure during Sintering. [11] studied physico-chemical investigations of high iron bauxite.

Guinean bauxite deposits have been the subject of several studies. The bauxites of the Sangarédi deposit were formed by the laterization of various parental rocks, including argillites, dolerites and marine sediments. Some of these were later modified by the diagenetic processes to form high-alumina chimogen varieties [12]. [13] addressed Petrography, Mineralogy, Geochemistry and Genesis of the Balaya bauxite deposits in the Kindia region. A physicochemical characterization of Débélé bauxite is addressed in [14]. Guinean Geology study is addressed in [15].

Concerning the Sangarédi bauxite deposits in Guinea, some physico-chemical characterization works were carried out, among which we can cite the recent work of [16] on the Petrological and Statistical Studies of the Limbiko Bauxite Deposit, a geochemical study of the Sangarédi deposit by [17]. [18] identified a wider range of parental rocks in the Boké-Sangarédi area, including Palaeozoic metasedimentary and magmatic rocks, as well as Cenozoic sediments. Mineralogical and Geochemical Characteristics of the Sangarédi Bauxite Deposits is investigated in [12]. The Sangaredi bauxites enrichment process is proposed in [19].

However, little scientific research exists on the physical and mechanical characterization of the Sangarédi bauxites deposit taking into account their litho-genetic type. To better characterize the physico-mechanical proprieties of the Bauxites type, several samplings depending on the depth must be realized. [20] shows the shear strength at a depth of more than 5 m is much larger than the material in the shallow layer close to the surface.

This paper presents a model of Physico-Mechanical Characterization of Bauxite and related rocks, taking into account their litho-genetic type. For each litho-genetic type, several samplings were done at different depth levels, and physical and mechanical characterization tests were carried out on each sample. The effect of depth of sampling on these physico-mechanical parameters was evaluated. Thus, an average of the values is made to obtain a representative value of the litho-genetic type, and at the end, a comparative study of the average value of the physico-

mechanical parameters of the different bauxite types was carried out. This paper is organized as follows. After the introduction section above, the Materials and Methods section is presented, in which the experimental method and devices that allow computing the physico-mechanical parameters of the bauxite types are explained. The main results are then presented, followed by the discussion. At the end, conclusions are presented

2. Materials and Methods

2.1. Sampling Method

Eights (8) mining pits, which varied in depth between 0.2 and 11 m, have been drilled in the study area. For each pit, bauxite samples of each litho-genetic type were collected at different depth levels. The bauxite samples were recorded and coded according to the pit number and depth of sampling. They were collected based on their color, structure and location within the study area. **Figure 1** shows the pits, the litho-genetic type of bauxites in each pit and the sampling procedure, and **Table 1** presents samples recorded for each bauxite type and the depth in which they were collected

2.2. Physical and Mechanical Characterization Techniques

In this subsection, we determined the water of absorption of the samples recorded in **Table 1**. The water of absorption is a physical parameter that gives the value of a product's susceptibility to let water pass in it once immersed in water. In this work, for all samples, the average weight of fired bauxite is measured, and that, when soaked in water for an hour, is also weighed [5]. We use the following relation computing water of absorption (WA).

$$WA(\%) = \frac{Sw - Fw}{Fw} \tag{1}$$

where Sw is the soaked weight, and Fw is the fired weight of samples.

Mechanical Characterization

Compressive Strength

The compressive strength is determined through uniaxial or triaxial compressive tests. Its value depends on the shape and dimensions of the specimen, its water content, and the loading speed. In this study, as in [12], we used the ASTM C99/C99M-09 standards for this analysis using Model CAT C46L2 Compressive device. One sample of each bauxite type (see **Table 1**) was subjected to a load between 500 N and 2500 N at a uniform loading rate. The specimen from each bauxite type had dimensions of 1 cm × 2 cm. The compressive strength is the highest stress sustained by the material before failure; its value is computed by Equation (2).

$$CS = \frac{P}{BW} \tag{2}$$

where P is the failure load (maximum compressive force applied on Sample), B,

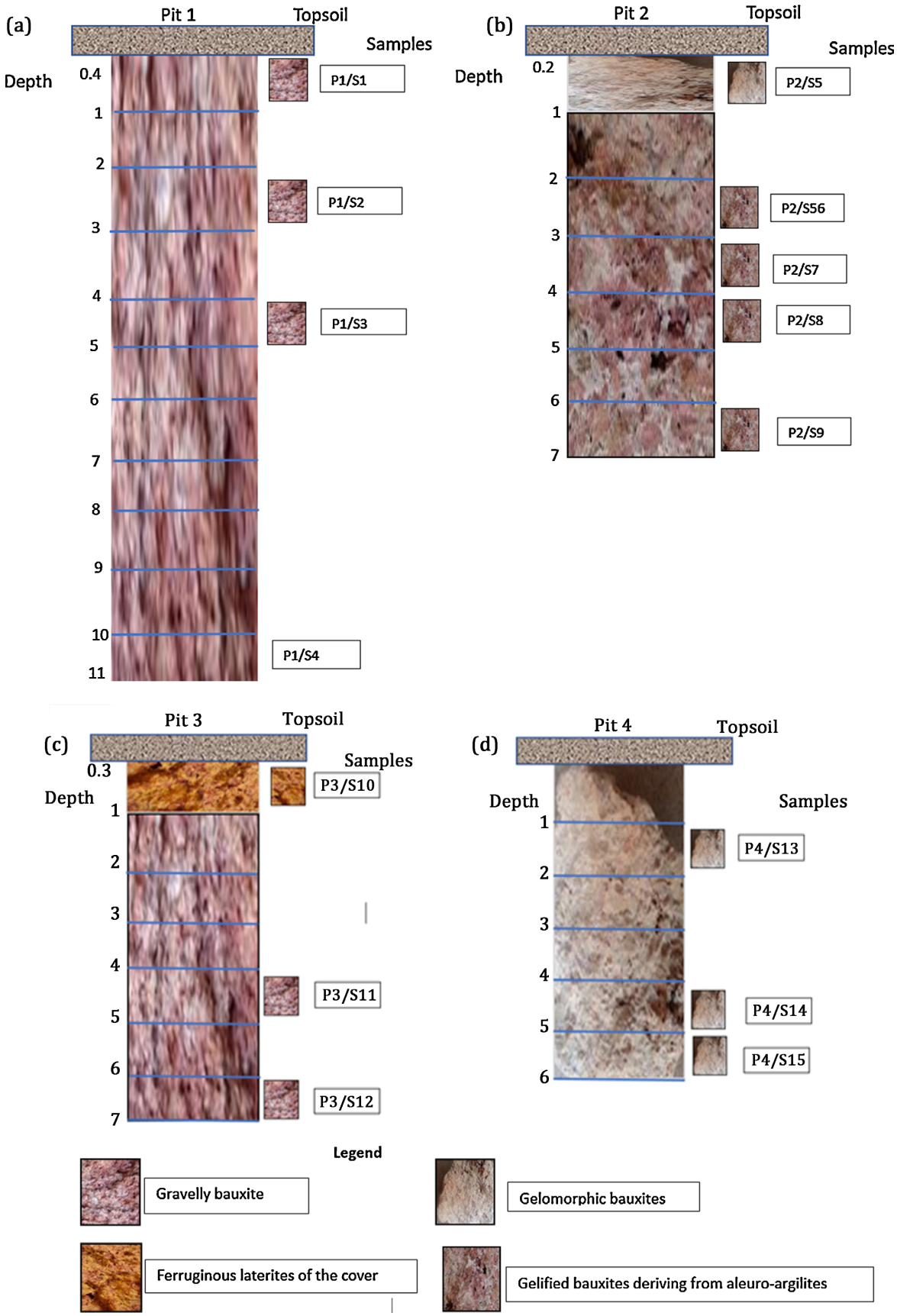
(a)
Pit 1
Topsoil
Samples
Depth
0.4
1
2
3
4
5
6
7
8
9
10
11
P1/S1
P1/S2
P1/S3
P1/S4
(b)
Pit 2
Topsoil
Samples
Depth
0.2
1
2
3
4
5
6
7
P2/S5
P2/S56
P2/S7
P2/S8
P2/S9
(c)
Pit 3
Topsoil
Samples
Depth
0.3
1
2
3
4
5
6
7
P3/S10
P3/S11
P3/S12
(d)
Pit 4
Topsoil
Depth
Samples
1
2
3
4
5
6
P4/S13
P4/S14
P4/S15
Legend
Gravelly bauxite
Gelomorphic bauxites
Ferruginous laterites of the cover
Gelified bauxites deriving from aleuro-argilites

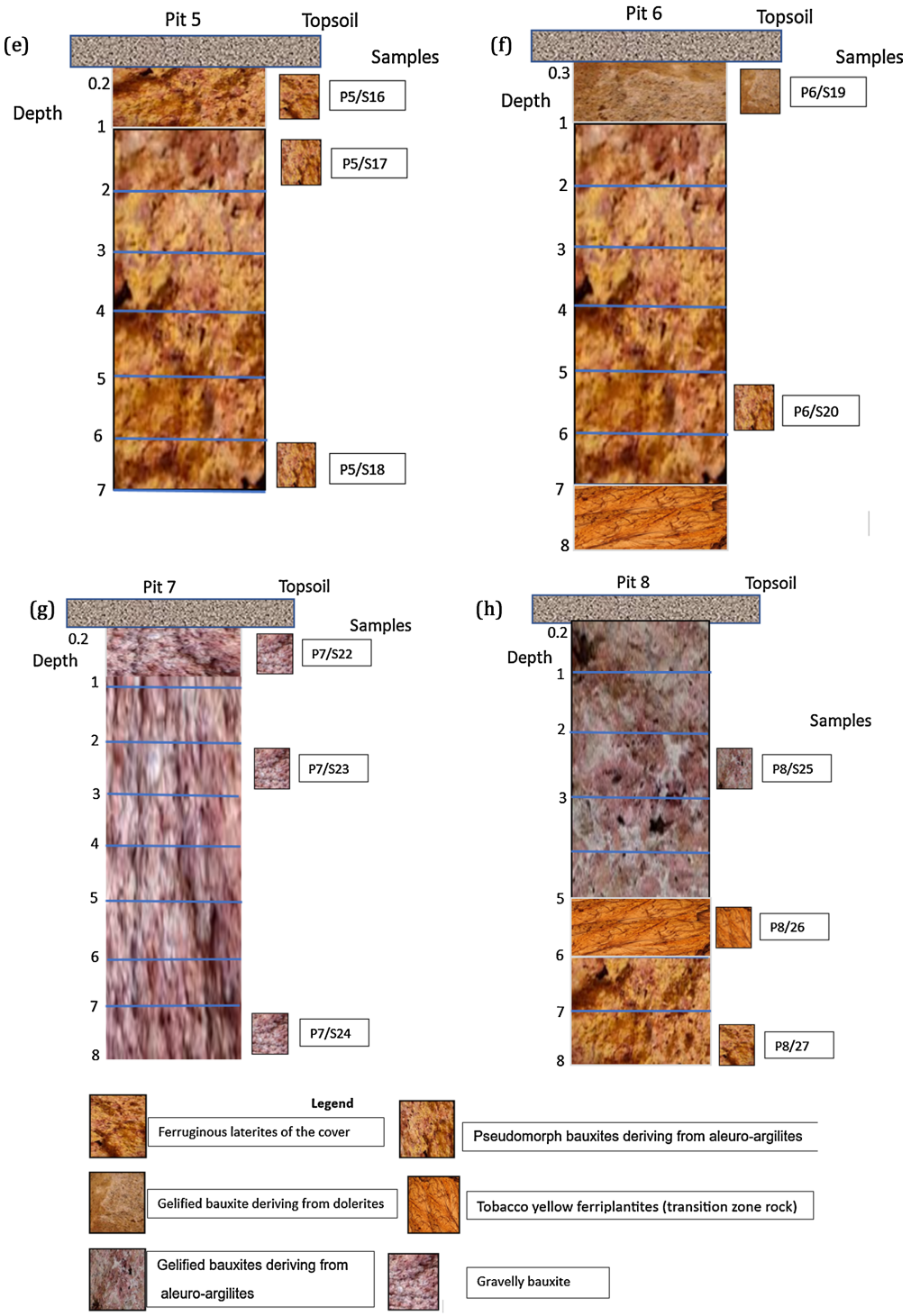

Figure 1. Pits, litho-genetic type of bauxite in each pit and the samples: (a) pit 1 gravelly bauxites (two samples collected); (b) pit 2 Gelomorphic bauxites (one sample collected) and Gelified bauxites deriving from aleuro-argilites (fours sapmles collected); (c) pit 3 Ferruginous laterites of the cover (one sample collected) and gravelly bauxite (two samples collected); (d) pit 4 Gelomorphic bauxite (three samples collected); (e) pit 5 Ferruginous laterites of the cover (one sample collected) and Pseudomorph bauxites deriving from aleuro-argilites (two samples collected); (f) pit 6 Gelified bauxite deriving from dolerites (one sample collected), Pseudomorph bauxites deriving from aleuro-argilites (one sample collected) and Tobacco yellow ferriplantites (transition zone rock) (on sample collected); (g) pit 7 Gravelly bauxites (three samples collected); (h) pit 8 Gelified bauxites deriving from aleuro-argilites (one sample collected), Tobacco yellow ferriplantites (transition zone rock) (on sample collected) and Ferruginous laterites of the cover (one sample collected).

Table 1. Samples were recorded for each bauxite type and the depth at which they were collected.

Geomorphic bauxites 		Gelified bauxites deriving from aleuro-argilites 		Gravelly bauxites 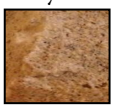		Pseudomorph bauxites deriving from aleuro-algilites 		Ferruginous laterites of the cover 	
Depth (m)	Samples code	Depth (m)	Samples code	Depth (m)	Samples code	Depth (m)	Samples code	Depth (m)	Samples code
[0.2 - 1.0]	P2/S5	[2 - 3]	P2/S6	[7 - 8]	P1/S1	[6 - 7]	P5/S18	[0.3 - 1.0]	P3/S10
[1 - 2]	P4/S13	[3 - 4]	P2/S7	[6 - 7]	P1/S2	[5 - 6]	P6/S20	[0.2 - 1.0]	P5/S16
[4 - 5]	P4/S14	[6 - 7]	P2/S8	[2 - 3]	P1/S3	[1 - 2]	P5/S17		
[5 - 6]	P4/S15	[4 - 5]	P2/S9	[4 - 5]	P3/S11				
		[2 - 3]	P8/S25	[6 - 7]	P3/S12				
				[10 - 11]	P1/S4				
				[0.2 - 1]	P7/S22				
				[2 - 3]	P7/S23				
				[0.4 - 1]	P7/S24<				

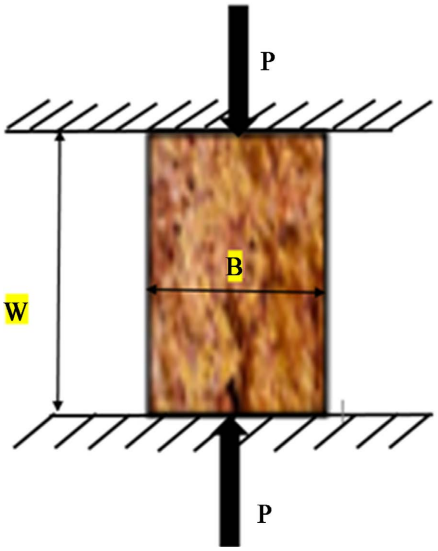

Figure 2. Schematic representation of a compression test.

and W are the width and height of the rectangular specimen. Figure 2 shows the schematic representation of a compression test with a specimen of one of the bauxite types.

Dynamic Tensile Strength

As bauxites are often subjected to dynamic loading during mining operations (case of sangarédi bauxite deposits exploitation), in this study, we performed a dynamic tensile test by spalling using a modified Hopkinson bar to evaluate the tensile strength of all the bauxites types in Table 1. The Hopkinson bar spalling

test is dedicated to the evaluation of the dynamic tensile strength of concrete and rock-like materials. The basic principle of dynamic tensile testing by spalling is to obtain a dynamic tensile stress field within a specimen which is loaded by an incident compression wave by the reflection of this wave on a free surface. The dimensions of the specimen are 120 mm long and 46 mm in diameter. The set-up involves a gaz-launcher, a cylindrical projectile with a large radius spherical end cap and a Hopkinson bar (**Figure 3**). The details of the design of this device can be found in [21] [22]. Tensile strength testing using a hardness tester was recently performed in [23].

The gaz-launcher releases the projectile that impacts the bar. An incident compressive wave in the form of a pulse A is generated (**Figure 4**). This pulse is propagated in the bar. When reaching the bar-sample interface, a part of the compressive wave is transmitted to the rock specimen B, while the other part of the wave is reflected in the bar because of the mechanical impedance discontinuity. The transmitted compressive pulse arrives at the free end of the specimen and

Figure 3. Experimental device of the dynamic tensile test by palling.

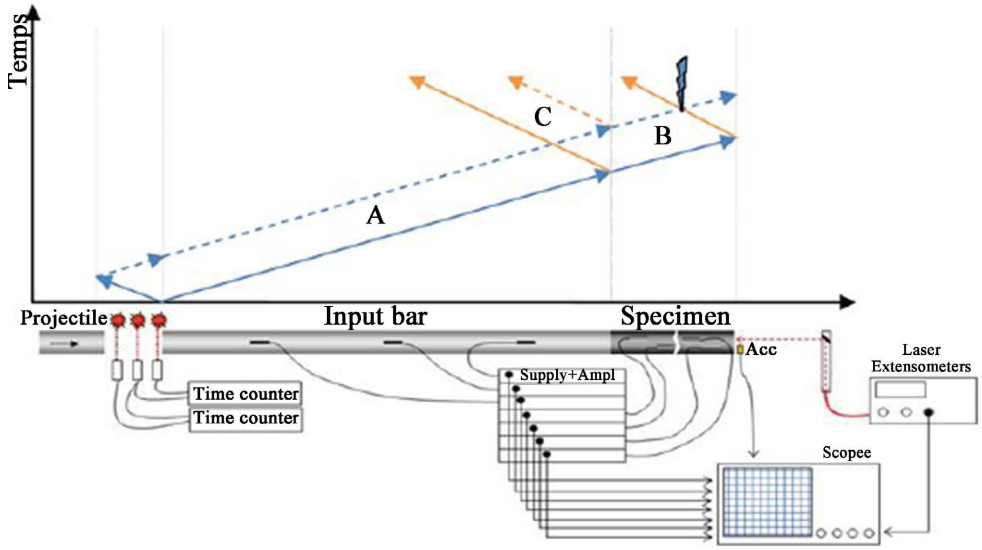

Figure 4. Schematic view of the instrumentation and wave propagation with time [21].

is reflected as a tensile pulse. When the reflected pulse exceeds the transmitted one in amplitude, a dynamic tensile loading develops in the core of the specimen, leading to its possible fragmentation [21]. Two strain gauges were placed directly on the bauxite specimen, respectively, at 100 mm and 50 mm from the free end of the sample (Figure 3) in order to monitor the time evolution of axial strain and deduce the axial stress before tensile damage (according to elastic theory) at two different locations in the specimen (Figure 3). A laser extensometer is also pointed directly toward the free back side of the sample to record the pullback velocity on the rear face.

Many approaches exist in the literature for the determination of the dynamic strength of specimen's subject to dynamic tensile test by spalling. Here, we used the approach of [24] based on the use of a linear acoustic approximation proposed by [25]. According to this approach, the dynamic tensile strength is given by

$$DTS = 1/2\rho C_o \Delta V_{pb} \tag{3}$$

where ρ is the material density, C_o is the one-dimensional wave speed of the incident wave, and ΔV_{pb} is the pullback velocity that corresponds to the difference between the maximum velocity and velocity at first rebound that is caused by tensile damage near the free surface. The compressive wave reaches first the gauge located at 100 mm from the free end and then the gauge at 50 mm from the free end, with a time shift measured so the speed of the incident wave can be estimated.

3. Results and Discussions

3.1. Physical and Mechanical Characterization Results

The results of the Physical and Mechanical Characterization of the bauxite type are presented in this section. Table 1 is completed by adding the water of absorption, compressive strength, and dynamic tensile strength (Tables 2-6).

Table 2. Physical and mechanical characterization results (water of absorption, compressive strength, and dynamic tensile strength) for Gelomorphic bauxites.

Geomorphic bauxites					
					
Sampling procedure		Water of absorption masse	Water of absorption volume	Compressive Strength	Dynamic Tensile Strength
Depth (m)	Samples code	WA (%) masse	WA (%) volume	CS (kgf/cm^2)	DTS (kgf/cm^2)
[0.2 - 1.0]	P2/S5	3.52	6.94	175	35
[1 - 2]	P4/S13	8.6	13.9	118.8	28.3
[4 - 5]	P4/S14	13	14.71	143.8	30
[5 - 6]	P4/S15	8.7	14.82	100	30
Average		8.5	12.6	134.4	30

Table 3. Physical and mechanical characterization results (water of absorption, compressive strength, and dynamic tensile strength) for Gelomorphic bauxites.

Gelified bauxites deriving from aleuro-argilites

Sampling procedure		Water of absorption masse	Water of absorption volume	Compressive Strength	Dynamic Tensile Strength
Depth (m)	Samples code	WA (%) masse	WA (%) volume	CS (kgf/cm^2)	DTS (kgf/cm^2)
[2 - 3]	P2/S6	8	13.51	110	33.3
[3 - 4]	P2/S7	6.43	11.86	155	39.3
[6 - 7]	P2/S8	7.8	12.73	95	33.7
[4 - 5]	P2/S9	5.7	10.72	150	38.9
[2 - 3]	P8/S25	6.9	11.77	151.3	38.7
Average		7	12.1	132.3	36.8

Table 4. Physical and mechanical characterization results (water of absorption, compressive strength, and dynamic tensile strength) for Gravelly bauxites.

Gravelly bauxites

Sampling procedure		Water of absorption masse	Water of absorption volume	Compressive Strength	Dynamic Tensile Strength
Depth (m)	Samples code	WA (%) masse	WA (%) volume	CS (kgf/cm^2)	DTS (kgf/cm^2)
[7 - 8]	P1/S1	5.6	9.63	125	43.4
[6 - 7]	P1/S2	5.68	11	103.1	36.6
[2 - 3]	P1/S3	8.3	15	178.7	28.3
[4 - 5]	P3/S11	11.92	19.54	80	26.6
[6 - 7]	P3/S12	7.8	13.73	69	26.6
[10 - 11]	P1/S4	12	22.27	-	26.7
[0.2 - 1]	P7/S22	3.92	7.68	92	40.3
[2 - 3]	P7/S23	7	12.01	175	53.3
[0.4 - 1]	P7/S24	10.53	16.93	81.3	36
Average		8.2	14.3	109.7	35.1

Table 5. Physical and mechanical characterization results (water of absorption, compressive strength, and dynamic tensile strength) for Pseudomorph bauxites deriving from aleuro-algilites.

Pseudomorph bauxites deriving from aleuro-algilites 					
Sampling procedure		Water of absorption masse	Water of absorption volume	Compressive Strength	Dynamic Tensile Strength
Depth (m)	Samples code	WA (%) masse	WA (%) volume	CS (kgf/cm^2)	DTS (kgf/cm^2)
[6 - 7]	P5/S18	10.7	20	121.9	23.3
[5 - 6]	P6/S20	6.2	10.45	69	36.7
[1 - 2]	P5/S17	4	7.59	98	26.7
Average		7	12.7	96.3	28.9

Table 6. Physical and mechanical characterization results (water of absorption, compressive strength, and dynamic tensile strength) for Ferruginous laterites of the cover (transition zone rock).

Ferruginous laterites of the cover 					
Sampling procedure		Water of absorption masse	Water of absorption volume	Compressive Strength	Dynamic Tensile Strength
Depth (m)	Samples code	WA (%) masse	WA (%) volume	CS (kgf/cm^2)	DTS (kgf/cm^2)
[0.3 - 1.0]	P3/S10	3.22	6.78	161	40
[0.2 - 1.0]	P5/S16	2.8	5.85	181.3	40
Average		3.0	6.3	171.2	40

3.2. Effect of Depth of Sampling on Water of Absorption, Compressive Strength and Dynamic Tensile Strength

- **Gelomorphic Bauxite**

Figure 5 shows the effect of depth of sampling on water of absorption, compressive strength, and dynamic tensile strength of gelomorphic bauxite. From depth interval [0.2 - 1] m (Figure 5(a)), we observed an inverse relation between compressive strength and water of absorption (water of absorption increases when compressive strength decreases) until intersection, while from depth interval [1 - 4] m, the two parameters have the same evolution (both increase). At the end of the depth interval [4 - 6] m, they also have the same trends (both decrease). In Figure 5(b), it is also observed that an inverse relation between dynamic tensile strength and water of absorption from depth interval [0.2 - 1.5] m. Unlike compressive strength, dynamic tensile strength keeps increasing constantly from

depth interval [1.5 - 6] m.

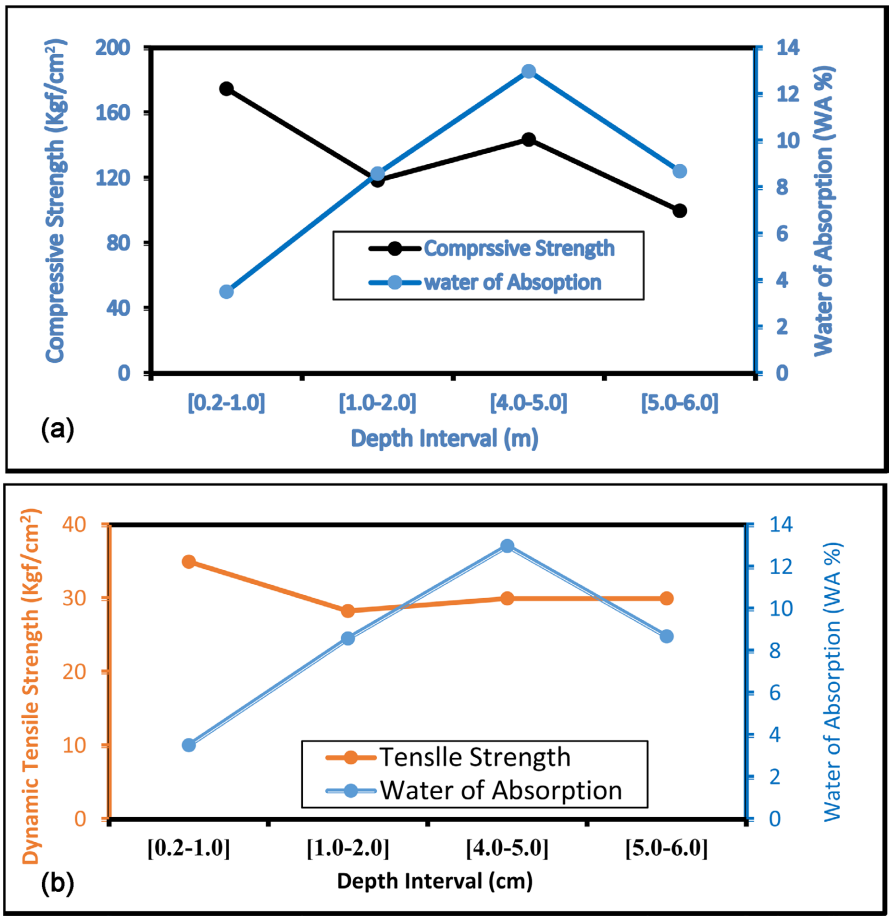

Figure 5. Effect of depth of sampling on water of absorption, compressive strength, and dynamic tensile strength for Gelomorphic bauxite.

- **Gelified Bauxites Deriving from Aleuro-Argilites**

In Figure 6(a), an inverse relation is observed between compressive strength and water of absorption from all de depth intervals. An increase in water of absorption leads to a decrease in compressive strength, while a decrease in water of absorption leads to an increase in compressive strength. The relation between dynamic tensile strength and water of absorption shows the same trends (Figure 6(b)).

- **Gravelly Bauxites**

Figure 7(a) shows an inverse relation between compressive strength and water of absorption from de-depth interval [7 - 8] m. From depth intervals ([6.0 - 7.0] [1.0 - 2.0]) m, the same evolution is observed for the two parameters (increases), while from depth interval [4.0 - 5.0] [6.0 - 7.0] m, the same decreases is observed for the two parameters. At the end, again, an inverse relation is observed from depth interval [0.4 - 1.0] m. Figure 7(b) shows the same trends between dynamic tensile strength and water of absorption.

- **Pseudomorph Bauxites Deriving from Aleuro-Algilites**

For the pseudomorph bauxites deriving from aleuro-algilites, compressive

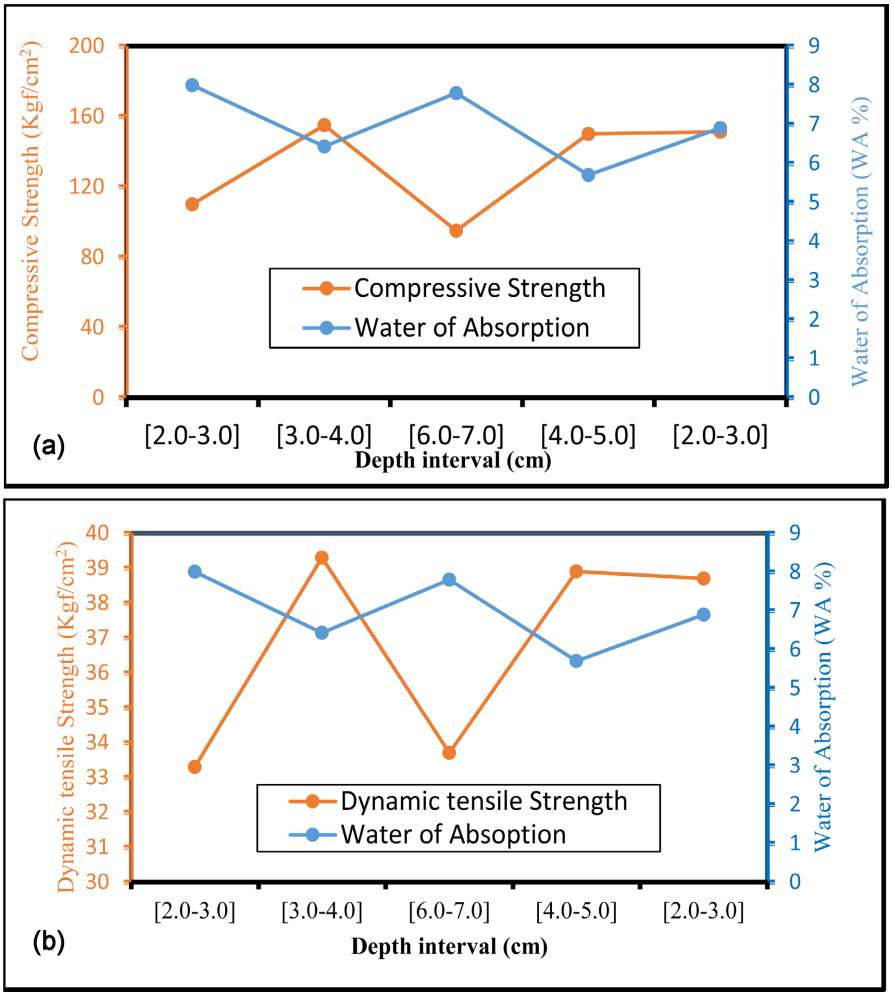

Figure 6. Effect of depth of sampling on water of absorption, compressive strength, and dynamic tensile strength for Gelified bauxites deriving from aleuro-argilites.

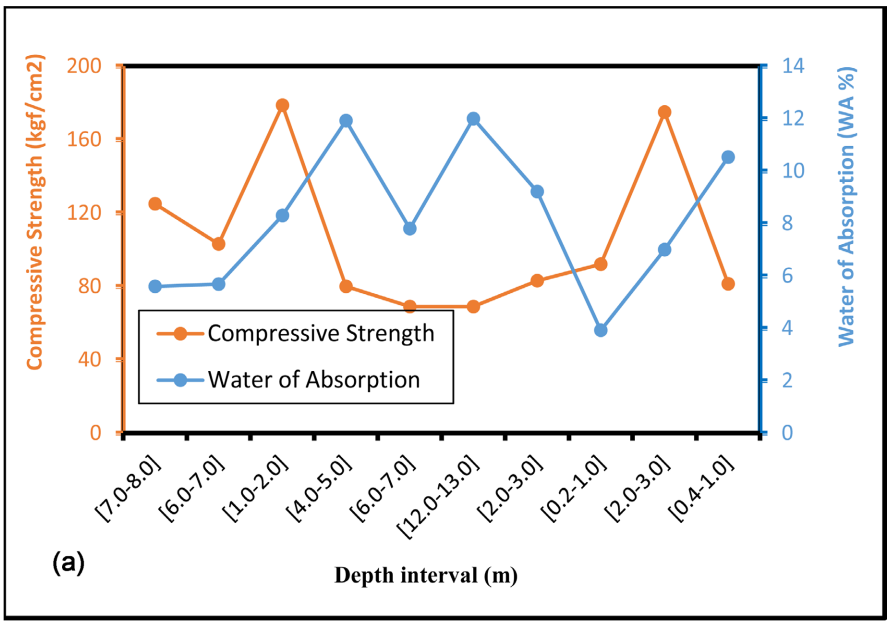

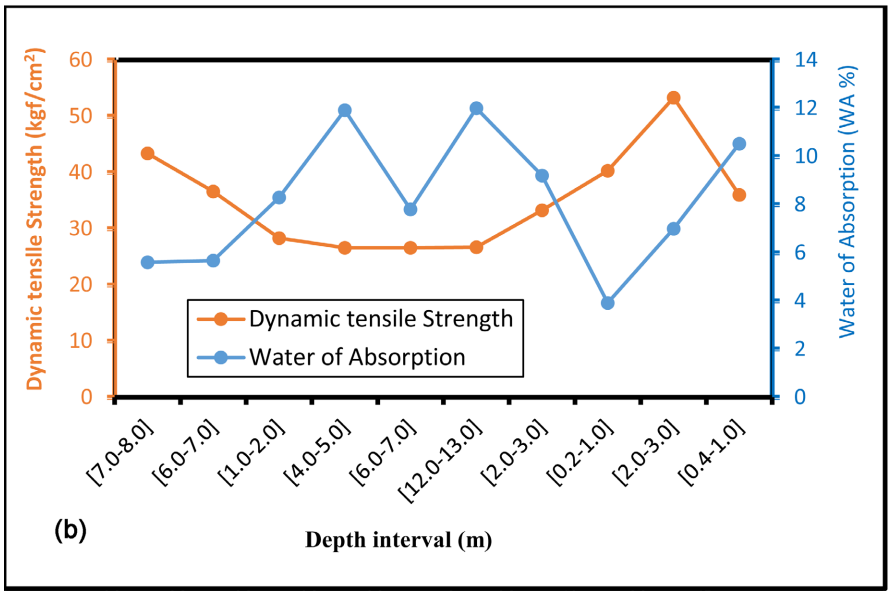

Figure 7. Effect of depth of sampling on water of absorption, compressive strength, and dynamic tensile strength for Gravelly bauxites.

strength and water of absorption have both a linear decrease over depth interval [6.0 - 7] and [5.0 - 6.0], while they have an inverse relation over depth interval [5.0 - 6.0] and [1.0 - 2.0] (Figure 8(a)). In Figure 8(b), it is observed the dynamic tensile strength and water of absorption have trends contrary to those in Figure 8(a). An inverse relation over depth interval [6.0 - 7] and [5.0 - 6.0] (a decrease of water of absorption leads to an increase of dynamic tensile strength). They have a linear decrease over depth interval [5.0 - 6.0] and [1.0 - 2.0].

- **Ferruginous Laterites of the Cover**

Ferruginous laterites of the cover are a rock of the transition zone between topsoil and bauxite types. Because it is found on the first layers after the topsoil, it can only be collected from a depth interval of [0.2 - 1] and [0.3 - 1]. An inverse relation between compressive strength and water of absorption is observed from all the depth intervals. A decrease of water of absorption leads to an increase of compressive strength (Figure 9(a)). The dynamic tensile strength and water of absorption relation show the same behavior (Figure 9(b)).

3.3. Comparison of the Physico-Mechanical Characteristics of the Different Bauxites Types Studied

From Tables 2-6, we represent the comparison of the physico-mechanical characteristics of the different bauxite types and transition zone rock studied. Figure 10 shows this comparison.

As it can be observed, the Ferruginous laterites of the cover (transition zone rock) have the lowest water of absorption value. This is explained by the fact it is the rock that occupies the first upper layer after the topsoil, so it lets surface water pass toward the water Table. It contains greater porosity compared to bauxites. The Ferruginous laterites of the cover also have the highest compressive strength

and dynamic tensile strength value (see Figure 10(b) & Figure 10(c)). This is because of the inverse relation between water of absorption and compressive strength and dynamic tensile strength, as illustrated in Figure 9(a) & Figure 9(b).

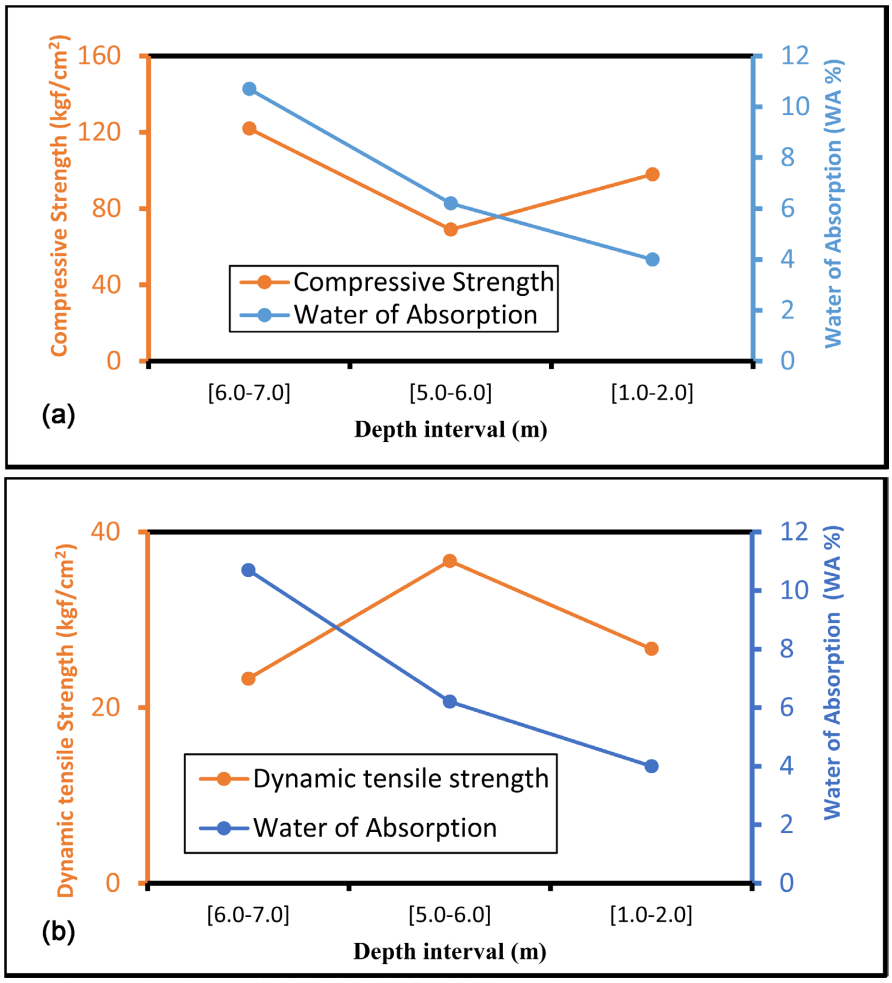

Figure 8. Effect of depth of sampling on water of absorption, compressive strength, and dynamic tensile strength for Pseudomorph bauxites deriving from aleuro-algilite.

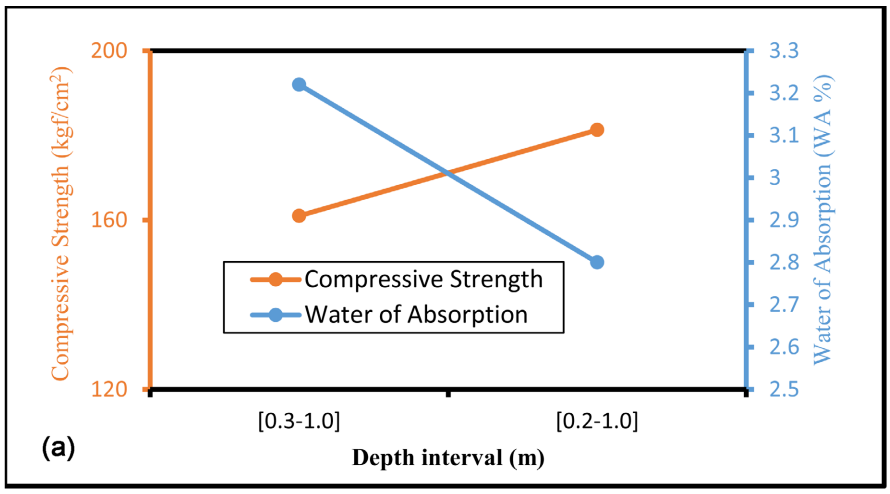

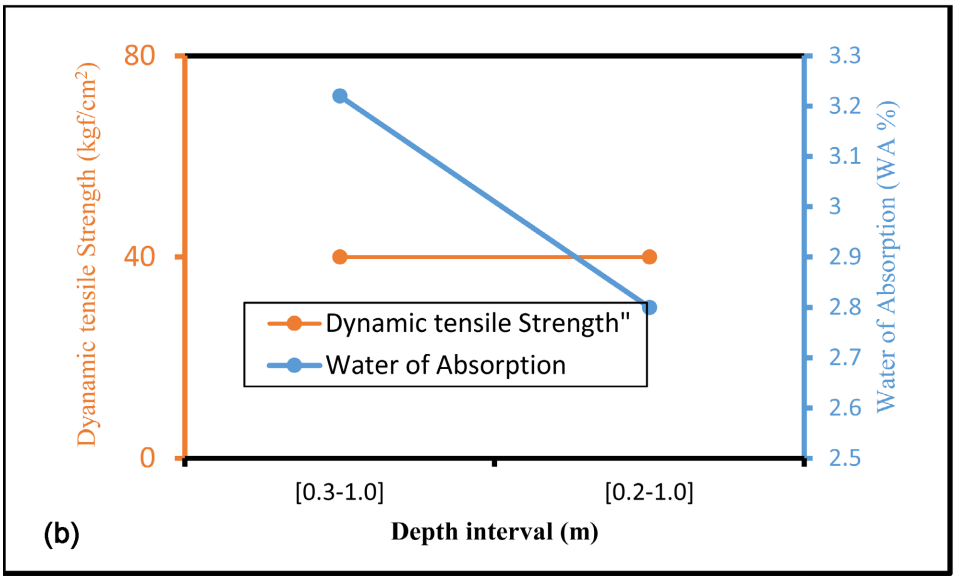

Figure 9. Effect of depth of sampling on water of absorption, compressive strength, and dynamic tensile strength for Ferruginous laterites of the cover (transition zone rock).

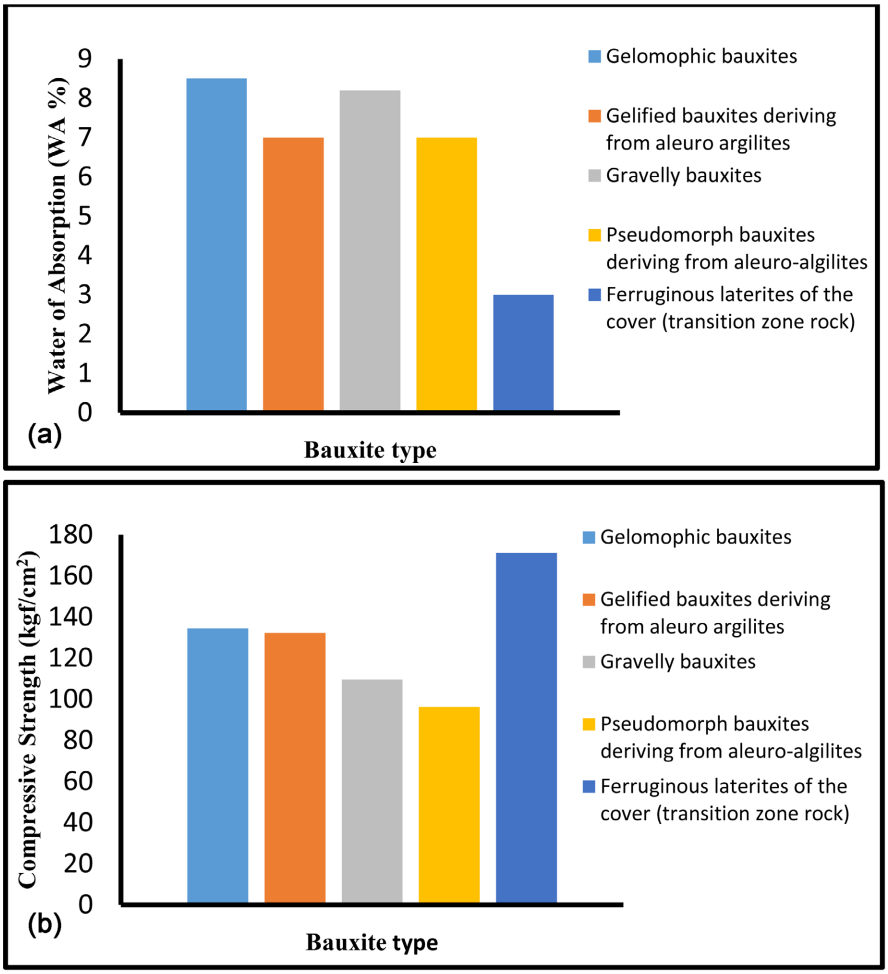

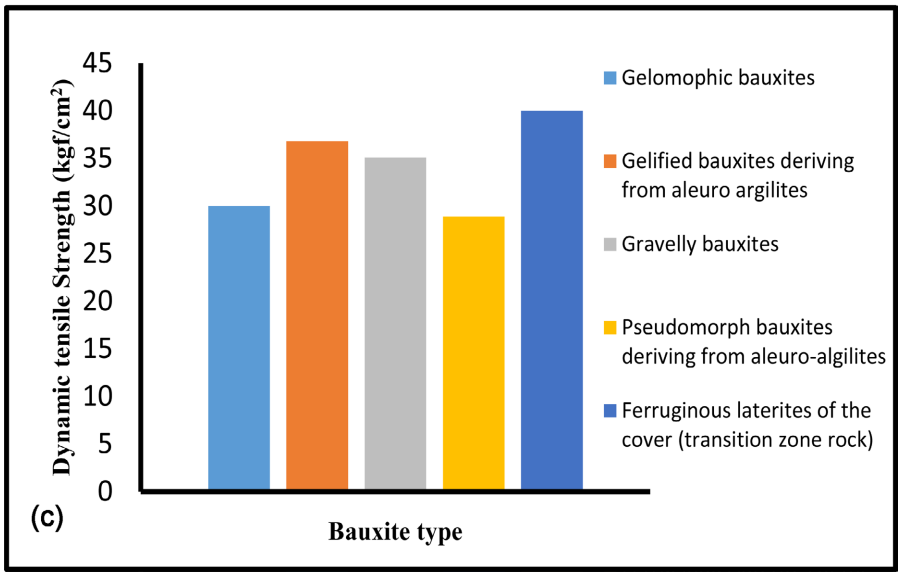

Figure 10. A comparison of the physico-mechanical characteristics of the different bauxite types and transition zone rock was studied. (a) water of absorption, (b) compressive strength, (c) dynamic tensile strength.

The Gelomorphic bauxites have the highest compressive strength value (Figure 10(b)), while Gelified bauxites deriving from aleuro-argilites have the highest dynamic tensile strength value (Figure 10(c)).

4. Conclusion

In this research, a model for the physico-mechanical characterization of Sangarédi bauxites according to their litho-genetic type is proposed. The following parameters: Water of Absorption, Compressive Strength and Dynamic Tensile Strength were computed for the type of the following bauxite: Gelomorphic bauxites, Gelified bauxites deriving from aleuro-argilites, Gravelly bauxites, Pseudomorph bauxites deriving from aleuro-algilite and Ferruginous laterites of the cover (transition zone rock). For each bauxite type, samples were collected at different layers from different depth levels. The compressive test, Dyanamic tensile, and water of absorption tests were carried out on all samples. For each bauxite type, an average value of the parameter obtained by each sample is made. The results showed that the physico-mechanical characteristics of bauxites depend on the depth of sample collection, and it is the average value of the parameters constitutes the representative values of the bauxite type. Finally, a comparative study of the average value of the physico-mechanical parameters of the different bauxite types was performed. The results showed the Ferruginous laterites of the cover (transition zone rock) have the highest compressive strength and dynamic tensile strength value (see Figure 10(b) & Figure 10(c)). The Gelomorphic bauxites have the highest compressive strength value (Figure 10(b)), while Gelified bauxites deriving from aleuro-argilites has the highest dynamic tensile strength value (Figure 10(c)).

Conflicts of Interest

The authors declare no conflicts of interest regarding the publication of this paper.

References

[1] Ministry of Mines and Geology (2020) Mining Potential Resources. https://mines.gov.gn/

[2] Sidiki, S. (2019) Bauxite Mining in the Boké Region (Western Guinea): Method Used and Impacts on Physical Environment. *European Journal of Sustainable Development Research*, **3**, em0087. https://doi.org/10.29333/ejosdr/5735

[3] Mouratidis, A. and Nikolidakis, P. (2020) Engineering Properties of Bauxite Residue. *International Journal of Sustainable Development and Planning*, **15**, 319-325. https://doi.org/10.18280/ijsdp.150308

[4] Zamanian, H., Ahmadnejad, F. and Zarasvandi, A. (2016) Mineralogical and Geochemical Investigations of the Mombi Bauxite Deposit, Zagros Mountains, Iran. *Geochemistry*, **76**, 13-37. https://doi.org/10.1016/j.chemer.2015.10.001

[5] Mamedov, V.I., Boufeev, Y.V. and Nikitine, Y.A. (2010) Geology of the Republic of Guinea. Ministry of Mines and Geology of the Republic of Guinea. Geoprospects LTD, University Moscow State Council.

[6] Tom, A., Djonga, P.N.D., Tsamo, C., Valery, H.G., Azangueu, J. and Noukelag, S.K. (2022) Structural Characterization of Bauxite Red Mud to Utilization in Ceramic Wall/roofing Tile: Effect of Temperature on Mechanical Properties and Physic-Chemical Stability. *Advances in Materials Physics and Chemistry*, **12**, 1-18. https://doi.org/10.4236/ampc.2022.121001

[7] Wei, F., Xing, M., Li, S., Shan, J. and Guan, B. (2020) Physical and Mechanical Properties of Epoxy-bauxite Mortar of High-Friction Surface Treatment. *Journal of Materials in Civil Engineering*, **32**, Article ID: 04020146. https://doi.org/10.1061/(asce)mt.1943-5533.0003201

[8] Jiang, J., Su, J., Ou, X., Weng, M. and Lü, X. (2021) Study on the Physical and Mechanical Properties of Bauxite Residue by Laboratory and Field *In-Situ* Tests. *Environmental Earth Sciences*, **80**, Article No. 377. https://doi.org/10.1007/s12665-021-09679-3

[9] Parhi, B.R., Sahoo, S.K., Sahu, M., Bishoyi, B.D., Mishra, S.C., Bhoi, B., *et al.* (2017) Physico-Chemical Investigations of High Iron Bauxite for Application of Refractive and Ceramics. *Metallurgical Research & Technology*, **114**, Article No. 307. https://doi.org/10.1051/metal/2017025

[10] Michel, R., de Bilbao, E. and Poirier, J. (2016) Recycling Bauxite Waste for the Mineral Industry: Phase Transformations and Microstructure during Sintering. *Waste and Biomass Valorization*, **9**, 1261-1271. https://doi.org/10.1007/s12649-016-9775-y

[11] Liu, X., Wang, Q., Zhang, Q., Feng, Y. and Cai, S. (2012) Mineralogical Characteristics of the Superlarge Quaternary Bauxite Deposits in Jingxi and Debao Counties, Western Guangxi, China. *Journal of Asian Earth Sciences*, **52**, 53-62. https://doi.org/10.1016/j.jseaes.2012.02.011

[12] Barry, A.D., Cissé, M., Parfait, M.M. and Hallarou, M.M. (2021) Mineralogical and Geochemical Characteristics of the Sangarédi Bauxite Deposit, Boké Region, Republic of Guinea. *Environmental and Earth Sciences Research Journal*, **8**, 11-22. https://doi.org/10.18280/eesrj.080102

[13] Sidibe, M. and Yalcin, M.G. (2019) Petrography, Mineralogy, Geochemistry and Genesis of the Balaya Bauxite Deposits in Kindia Region, Maritime Guinea, West Africa.

Journal of African Earth Sciences, **149**, 348-366. https://doi.org/10.1016/j.jafrearsci.2018.08.017

[14] Balde, M.Y., Djangang, C.N., Diallo, R.B., Blanchart, P. and Njopwouo, D. (2021) Physicochemical Characterisation for Potential Uses as Industrial Mineral of Bauxite from Débélé, Guinea. *Journal of Materials Science and Chemical Engineering*, **9**, 9-22. https://doi.org/10.4236/msce.2021.93002

[15] Aristide Zé, P., Tsamo, C. and Kamga, R. (2018) Characterization of Minim-Martap Bauxite and Its Extracted Alumina. *Journal of Advanced Chemical Sciences*, **4**, 598-600. https://doi.org/10.30799/jacs.198.18040402

[16] Diallo, A.K., Conte, M.S.M., Kaba, O.B., Soumah, A. and Camara, M. (2023) Petrological and Statistical Studies of the Limbiko Bauxite Deposit, Republic of Guinea. *International Journal of Geosciences*, **14**, 351-376. https://doi.org/10.4236/ijg.2023.144020

[17] Mamedov, V.I., Chausov, A.A. and Kanishev, A.I. (2011) Formation Stages of the Unique Sangaredi Bauxite-Bearing Group, Futa Jallon-Mandingo Province, West Africa. *Geology of Ore Deposits*, **53**, 177-201. https://doi.org/10.1134/s1075701511030044

[18] Zhang, R., Gong, E., Wang, G. and Peng, W. (2018) Mineralization Patterns and Conditions of Lateritic Gibbsite Bauxite in Guinea. *Advances in Geoscience*, **1**, 38-48.

[19] Beavogui, M.C., Balmaev, B.G., Kaba, O.B., Konaté, A.A. and Loginova, I.V. (2022) Bauxite Enrichment Process (Bayer Process): Bauxite Cases from Sangaredi (Guinea) and Sierra Leone. *AIP Conference Proceedings*, **2456**, Article ID: 020003. https://doi.org/10.1063/5.0074812

[20] Silva, F.A.N.G., Sampaio, J.A., Garrido, F.M.S. and Medeiros, M.E. (2011) Study on the Characterization of Marginal Bauxite from Pará/Brazil. In: Lindsay, S.J., Ed., *Light Metals* 2011, Springer, 13-18. https://doi.org/10.1007/978-3-319-48160-9_2

[21] Forquin, P. and Erzar, B. (2009) Dynamic Fragmentation Process in Concrete under Impact and Spalling Tests. *International Journal of Fracture*, **163**, 193-215. https://doi.org/10.1007/s10704-009-9419-3

[22] Erzar, B. and Forquin, P. (2009) An Experimental Method to Determine the Tensile Strength of Concrete at High Rates of Strain. *Experimental Mechanics*, **50**, 941-955. https://doi.org/10.1007/s11340-009-9284-z

[23] Schuler, H., Mayrhofer, C. and Thoma, K. (2006) Spall Experiments for the Measurement of the Tensile Strength and Fracture Energy of Concrete at High Strain Rates. *International Journal of Impact Engineering*, **32**, 1635-1650. https://doi.org/10.1016/j.ijimpeng.2005.01.010

[24] Sebayang, M.D. and Putra, R.M. (2024) Analysis of Hardness, Crystal Structure, and Tensile Strength by Treatement with Variation of Welding Current Strengh Gtaw Material SS 316L. *ARPN Journal of Engineering and Applied Sciences*, **19**, 541-545.

[25] Novikov, S.A., Divnov, L.L. and Ivanov, A.G. (1966) Study of Rupture of Steel, Aluminum and Copper under Exploisif Loading. *Fizika Metallov Metallovedeniye*, **21**, 23-32.